Frequency Diverse Array Radar Data Processing

Yunhan Dong
National Security and ISR Division
Defence Science and Technology Group
Australia
yunhan.dong@dst.defence.gov.au

***Abstract*—The frequency diverse array (FDA) radar has recently been proposed. However, what left behind is how the FDA data should be correctly, efficiently and systematically processed to maximise its full potential and capacity of search and detection. This paper fills the gap. It shows that overall the processing of the FDA data is even simpler and faster than the processing of the conventional phased-array (CPA) radar to complete wide-area search and detection without a need of electronic scan and repeat pulse transmission and reception. The ambiguous range is resolved without using multiple pulse repetition frequencies (PRFs). This not only greatly simplifies the radar's design and operation but also makes radar quieter and stealth.**

Keywords—frequency diverse array; radar signal processing; radar waveforms.

I. INTRODUCTION

Frequency diversity technology has recently been proposed and possibly applied to radar systems [1-7]. Having had its roots in wireless telecommunications, it is more popularly discussed in applications for multi-input multi-output (MIMO) radar systems [8, 9]. However, more and more studies on frequency diverse array (FDA) radar have been published in recent years. Wang published two review papers on FDA radar where 125 and 60 papers, respectively (there were overlaps though), were cited [10, 11]. Among those authors, Antonik, Wicks, Griffiths and Baker [1] were some of those who initially introduced this radar technology. Differing from its conventional phased-array (CPA) counterpart, the FDA employs pulsed continuous-wave (CW) waveforms with some frequency increment across array channels / elements to generate a range, angle and time dependent beam pattern [2, 12, 13] that may have some advantages and different features over the CPA counterpart.

While FDA radars have been widely studied and reviewed [10], characteristics, features, advantages as well as limitations of an FDA radar have not been reported thoroughly. The most important part being left behind is how the FDA data should be systematically and efficiently processed to explore its full potential and capacity in terms of search and detection. Some claimed advantages, such as achieving the same signal-to-noise ratio (SNR) improvement as the CPA radar and range-ambiguous clutter suppression, were not true. Some data processing techniques, notably, the pulse compression and beamforming, were insufficient or not necessary. The paper focuses more on the systematic processing of the FDA data on receive. Techniques analogous to those of the CPA data processing are presented. It shows that overall the processing the FDA data is faster and simpler than that of CPA data, but not the verse versa as suggested by most references. The ability of resolve range ambiguity without using multiple PRFs is demonstrated.

II. FDA DATA PROCESSING

A. Beamforming

In principle there could be two ways to carried out the FDA aperture synthesis and beamforming. The first way is to separate frequency components in each receiving channel (assuming the separation can be perfectly implemented), synthesise each frequency component across the whole array and then combine all frequency components coherently. The second way is to treat the received waveforms in each receiving channel as a whole and synthesise all channels appropriately. We can show that the results of these two ways are identical [14]. In fact, the perfect frequency separation cannot be implemented on receive using bandpass filters for short pulses. We use the second way for the beamforming and data processing.

Consider a linear one-dimensional (1D) FDA consisting of $N+1$ independent transceivers (channels, N is an even number) spaced by d in the azimuth direction ($d \le \lambda_0/2$, λ_0 is the wavelength of the carrier frequency f_0). Each channel is assigned a unique CW waveform with a frequency increment Δf ($N\Delta f << f_0$, so it is a narrowband system). The FDA radar 'steers' at the boresight direction (i.e. the $(r,0,0)$ direction in the $r\theta\phi$ polar coordinate system). The received signal in the k^{th} channel echoed by a point target or a clutter patch with a unit reflection coefficient located at (r_0,θ,ϕ) can be written as,

$$\gamma_{k,u}(r,\theta,\phi) = g^2(\theta,\phi) \sum_{n=-N/2}^{N/2} \exp\left(j\frac{2\pi f_n}{c}(2r+(n+k)d\vartheta) \right) \quad (1)$$

where $\vartheta = \cos\theta\sin\phi$; $f_n = f_0 + n\Delta f$, $\Delta f = 1/T$ and T is the pulse width, so waveforms in FDA channels are mutually orthogonal [5, 6]. Function $g(\theta,\phi)$ is the one-way individual transceiver directional gain pattern which is reciprocal for emission and receive, and is assumed to be identical for all channels ($g(\theta,\phi)\equiv 1$ is assumed hereafter for simplicity).

After focusing (focusing at r is achieved by a time delay of $\Delta t = 2r/c$), the signal received by the k^{th} channel is,

$$\gamma_k(\theta,\phi) = \sum_{n=-N/2}^{N/2} \exp\left(j\frac{2\pi f_n}{c}(n+k)d\vartheta \right) \quad (2)$$

Summing up all channels gives,

$$\Gamma(\theta,\phi) = \sum_{k=-N/2}^{N/2} \gamma_k(\theta,\phi) = \sum_{k=-N/2}^{N/2}\sum_{n=-N/2}^{N/2} \exp\left(j\frac{2\pi f_n}{c}(n+k)d\vartheta \right) \quad (3)$$

Since the frequency diversity is small compared to the carrier frequency, $N\Delta f << f_0$ (a narrowband system), f_n can be replaced by f_0 in (3), giving,

$$\Gamma(\theta,\phi) \approx G_0^2(\theta,\phi) \quad (4)$$

$$G_0(\theta,\phi) = \sum_{n=-N/2}^{N/2} \exp\left(j\frac{2\pi f_0}{c}nd\vartheta \right) = \frac{\sin\left((N+1)\pi\frac{f_0}{c}d\vartheta \right)}{\sin\left(\pi\frac{f_0}{c}d\vartheta \right)} \quad (5)$$

Readers can verify that there are essentially no any noticeable differences between the beamformed patterns given by the exact formula (3) and the approximation (4) for a narrowband case. Actually (4) is identical to the well-known two-way CPA beam pattern.

B. *FDA Data Processing*

The received signal in the k^{th} channel with respect to time can be written as

$$\gamma_{k,u}(t) = A\sum_{n=-N/2}^{N/2} \exp\left(j2\pi f_n(t-\Delta t) + j\frac{2\pi f_n}{c}(n+k)d\vartheta \right) \quad (6)$$

where A is a complexed value representing amplitude of the target reflection coefficient (the target is located at (r_0,θ,ϕ)); $\Delta t = 2r_0/c$ is the round trip time delay for unambiguous range r_0.

Unlike the CPA radar whose emission is coherent and has a constant time-angle pattern, the FDA emission is non-coherent and has a varying time-angle-range pattern [2, 10, 12, 13]. Therefore, the processing of the FDA radar needs focusing to 'steer' radar beam on to the location of interest. The focusing is to multiply a phase term of $\exp\left(-j2\pi f_n\left(2r+(n+k)d\vartheta\right)/c\right)$ to focus at (r,θ,ϕ) for the k^{th} receiving channel and frequency component of f_n. Because data received by a range bin is normally collected after a time delay of Δt, it means the radar has automatically focused at $(r_0,0,0)$, where $\Delta t = 2r_0/c$. If $(r_0,0,0)$ is the location of interest, there is no extra focusing processing required. However, if the location of interest is off the boresight, for instance, if (r_0,θ,ϕ) is the location of interest, then an extra phase of $\exp\left(-j2\pi f_n(n+k)d\vartheta/c\right)$ is required for the k^{th} channel and frequency f_n, so that the focusing point is changed from the point $(r_0,0,0)$ to point (r_0,θ,ϕ). The problem is that each receiving channel contains $N+1$ frequencies, and hence the above focusing processing is not straightforward as the received individual frequency components in a range bin are unknown. When the time delay Δt and the carrier frequency are excluded from (6), the received baseband signal in the k^{th} channel is,

$$\gamma_k(t) = A\sum_{n=-N/2}^{N/2} \exp\left(j2\pi n\Delta ft + j\frac{2\pi f_n}{c}(n+k)d\vartheta \right) \quad (7)$$

For a narrowband system, (7) can be simplified to,

$$\gamma_k(t) = A\exp\left(j\frac{2\pi}{\lambda_0}kd\vartheta \right)\sum_{n=-N/2}^{N/2} \exp\left(j2\pi n\Delta ft + j\frac{2\pi}{\lambda_0}nd\vartheta \right) \quad (8)$$

Therefore, for an orientation (θ,ϕ), the pulse compression processing is identical for all channels, with a matched filter of,

$$h(t,\theta,\phi) = \sum_{n=-N/2}^{N/2} \exp\left(j2\pi n\Delta ft + j\frac{2\pi}{\lambda_0}nd\vartheta \right) \qquad -T/2 \le t \le T/2 \quad (9)$$

Let,

$$\Delta t_\vartheta = \frac{d\vartheta}{\lambda_0\Delta f} \quad (10)$$

Equation (9) can be write as,

$$h(t,\theta,\phi) = \sum_{n=-N/2}^{N/2} \exp\left(j2\pi n\Delta f(t+\Delta t_\vartheta) \right) = h(t+\Delta t_\vartheta,0,0) \quad (11)$$

Note that (11) is important and interest as it shows that the matched filter $h(t,\theta,\phi)$ for an orientation (θ,ϕ) is a circularly rotated copy (by the amount of Δt_ϑ) of the matched filter $h(t,0,0)$ for the boresight direction. According to the property of convolution, if,

$$q(t) = \int_{-T}^{T} h(\tau,\theta,\phi)h^*(t-\tau,0,0)d\tau \quad (12)$$

then,

$$q(t-\Delta t_\vartheta) = \int_{-T}^{T} h(\tau,\theta,\phi)h^*(t-(\tau+\Delta t_\vartheta),0,0)d\tau \quad (13)$$

Equations (12) and (13) indicates that the pulse compression processing for an orientation (θ,ϕ) can be implemented by the pulse compression processing using a unified matched filter $h(t,0,0)$. However, the resulted range t is being circularly advanced ($\Delta t_\vartheta > 0$) or delayed ($\Delta t_\vartheta < 0$), i.e. the range of target is being shifted if $\vartheta \neq 0$ as the result of using the unified filter $h(t,0,0)$. This greatly saves the computational time for the pulse compression processing. Instead of using orientation-dependent matched filters to repeat the pulse compression, a single unified pulse compression is sufficient. After beamforming determines the bearing of the target, the range shift amount Δt_ϑ can also be determined, and the correct range is measured accordingly. The output of pulse compression by the use of the unified matched filter for the k^{th} channel is,

$$y_k(t) = A\exp\left(j\frac{2\pi}{\lambda_0}kd\vartheta \right)q(t-\Delta t_\vartheta) \qquad k = -N/2,\cdots,0,\cdots,N/2 \quad (14)$$

Finally, to line up the signals from all $N+1$ channels to focus at (r,θ,ϕ) we need to use a spatial steering vector of,

$$\mathbf{v}_s(\theta,\phi)=\frac{1}{\sqrt{N+1}}\left[1 \quad \exp(-j2\pi d\vartheta/\lambda_0) \quad \cdots \quad \exp(-j2\pi Nd\vartheta/\lambda_0)\right]^H \tag{15}$$

where the superscript H denotes complex conjugate transpose. Finally the pulse-compressed, aperture-synthesised and beamformed output is,

$$y_{out}(t,\theta,\phi)=\mathbf{v}_s^H(\theta,\phi)\mathbf{y}(t) \tag{16}$$

where $\mathbf{y}(t)=\left[y_{-N/2}(t) \quad \cdots \quad y_0(t) \quad \cdots \quad y_{N/2}(t)\right]^T$ and the superscript T denote transpose.

The spatial processing given by (16) is exactly the same as the spatial processing of the CPA data and can be implemented by the fast Fourier transform (FFT). The difference is that for the CPA radar, if transmission steers at the boresight direction, the illumination off the boresight direction is only by the array's sidelobes. Therefore, in general the CPA radar needs to electronically scan its beam for search and detection in different directions. However, there is no need for the FDA radar to do so, and the steering focusing is achieved by processing the same received data. The intensity of the received signal is independent of the signal arrival (θ,ϕ), under the assumption of the antenna element directional gain $g(\theta,\phi)=1$. In reality, the region is limited by the antenna element directional gain $g(\theta,\phi)$, the same as the CPA array's electronic scan region.

Since the FDA is a narrowband system, for the Doppler processing, the same temporal steering vectors can be used as if the radar is a narrowband CPA radar. Accordingly, the temporal steering vector of FDA is the same as of CPA. For a coherent processing interval (CPI) dataset, the associated temporal steering vector is,

$$\mathbf{v}_t=\frac{1}{\sqrt{M+1}}\left[1 \quad \exp\left(-j2\pi f_d/f_{PRF}\right) \quad \cdots \quad \exp\left(-j2\pi Mf_d/f_{PRF}\right)\right]^T \tag{17}$$

where $-f_{PRF}/2\le f_d\le f_{PRF}/2$ is the target Doppler frequency to be searched, f_{PRF} is the radar's pulse repetition frequency (PRF), $M+1$ is the number pulses in a CPI, and $f_d=-2v_a/\lambda_0$ where v_a is the target's radial velocity.

III. Detection and Identification of Range-Ambiguous Targets

For a radar operated in medium to high PRF modes, range can be ambiguous. This means that echoes from distant targets illuminated by previous pulses can be received by the current pulse repetition interval (PRI), resulting in the so-called range-ambiguous targets. In general, different PRFs have to be used to resolve this range-ambiguous issue. This complexes radar schedules, increases radar load and also increases the exposure of the radar.

It is possible for FDA radar to identify the true range of targets without using multiple PRFs. Since the transmission of FDA is non-coherent and channel frequencies are orthogonal, the combined waveforms can be totally different once an initial random phase is coded to each frequency. The random phase coded pulse m may be defined as,

$$s_m(t)=\sum_{n=-N/2}^{N/2}\exp\left(j2\pi(f_0+n\Delta f)(t-mT_r)+j\varphi(n,m)\right) \qquad -T/2\le t\le T/2 \tag{18}$$

where $0\le\varphi(n,m)\le 2\pi$ is a pseudo-random phase. As an example, Figure 1 shows the cross-correlation of two FDA pulses compared to the auto-correlation of an FDA pulse.

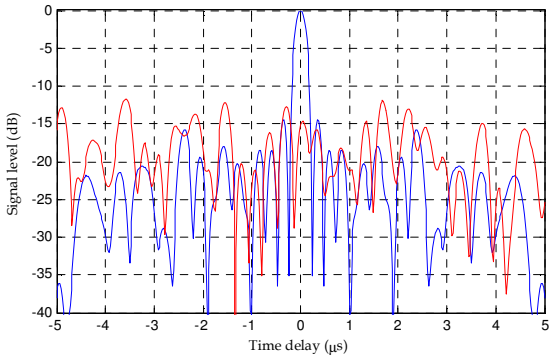

Figure 1: Autocorrelation of an FDA pulse and the cross-correlation of two FDA pulses. The waveforms are random phase coded as given by (18) ($N+1=41$, $T=10\,\mu$s and $\Delta f=100$ kHz).

When the received range samples undergo pulse compression, the target illuminated by the pulse matching with the pulse used in the pulse compression receives a coherent processing gain of $10\log_{10}(N+1)$ dB whereas the target illuminated by other pulse fails to receive this coherent processing gain. Likewise, the Doppler processing provides a coherent gains of $10\log_{10}(M+1)$ dB. Therefore, for the same target, its output SINR can be $10\log_{10}[(N+1)(M+1)]$ dB higher if the corresponding pulses are used in the pulse compression and Doppler processing compared to the use of non-corresponding pulses. In other words, for the same received data snapshot, different pulses should be used in pulse compression, so that all targets in either unambiguous range or ambiguous range can be detected and their true range determined.

The above statement is slightly over claimed. Realistically, two noise-like pulses with the same carrier frequency and same bandwidth should be treated as interference signals mutually. The cross-correlation, in terms of peak-to-sidelobe level (PSL), has a lower boundary of $10\log_{10}(N+1)$ dB which represents the best achievable isolation [15]. In general the peak of the cross-correlation is often higher than this theoretically lower bound (the lower bound is the mean value). The theoretically achievable isolation for the above example is $10\log_{10}41=16.1$ dB (the mean) and the actual isolation achieved is about 12 dB (the highest peak). However, this does demonstrate the use of the random-phase coded FDA waveforms to resolve the range-ambiguous targets and determine the true range of targets. The autocorrelation represents the result of pulse compression with the matched

pulse whilst the cross-correlation represents the result of pulse compression with an unmatched pulse.

In general, the FDA radar needs to refocus at $(r_0 + kr_{\max}, \theta, \phi)$ rather than (r_0, θ, ϕ) for detecting a target located at $(r_0 + kr_{\max}, \theta, \phi)$, where $r_{\max} = cT_r/2$, T_r PRI, i.e. $T_r = 1/f_{PRF}$ and $k = 1,2,\cdots$ is the order of range-ambiguity. However, if $\mathrm{mod}(n\Delta f, f_{PRF}) = 0$, for $n = 0,\pm 1,...,\pm N/2$, The focuses at $(r_0 + kr_{\max}, \theta, \phi)$ and (r_0, θ, ϕ) are the same. So there is no need of extra focus.

IV. Simulation

To demonstrate, a scenario is simulated using the geometric optics. Since the Doppler processing and clutter suppression/cancellation are well known, they are not included in the simulation, and only single-pulse data were generated. The thermal white Gaussian noise is the only undesired signal considered in the simulation.

Parameters used in the simulation are given in Table 1. The method of geometric optics was used in the simulation, i.e., waveforms transmitted by channels were treated separately according to channels' positions and targets' locations. The returned waveforms were than combined before adding the thermal noise.

Table 1: FDA and target parameters used in the simulation

	FDA Parameters
Carrier frequency, f_0	1.25 GHz (L-band)
Number of channels, $N+1$	41
Channel interval, d	Half wavelength
Pulse width, T	10 μs
Frequency diversity, Δf	100 kHz (linear) with a random initial phase
PRF	1500 Hz
Target parameters	
Target 1	49 km range, 30 deg azimuth
Target 2	51 km range, 0 deg azimuth
Target 3	150 km range, -30 deg azimuth

The data collection geometry is depicted in Figure 2. According to the FDA parameters, the maximum unambiguous range is 100 km. Therefore, Targets 1 and 2 are range-unambiguous targets whereas Target 3 is a range-ambiguous target, and its apparent range is 50 km.

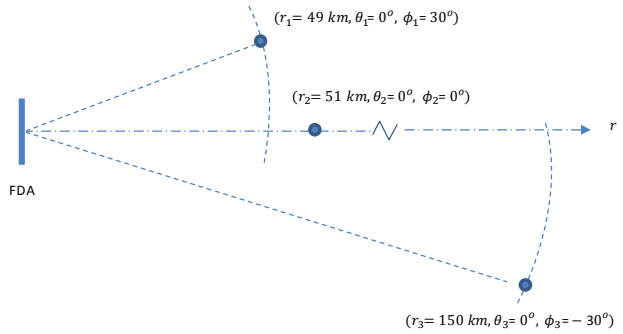

Figure 2: Geometry of FDA data collection.

The simulated raw data are shown in Figure 3 which is a noise dominant image as the SNR in the raw data for all three targets were assumed to be –10 dB.

After pulse compression using the range-unambiguous matched filter (the current pulse) and beamforming, the processed data is shown in Figure 4. It can be seen that both the range-unambiguous targets are detected: Target 1 ($r = 48.625$ km and $\cos\theta \sin\phi = 0.5$) and Target 2 ($r = 51$ km and $\cos\theta \sin\phi = 0$). Since Target 1 is off the boresight direction, its range has been shifted. The associated range shift in time, according to (10) is 2.5 μs, i.e. 0.375 km in range. Hence we determine the true range of Target 1 to be 49 km, consistent with the given simulation conditions.

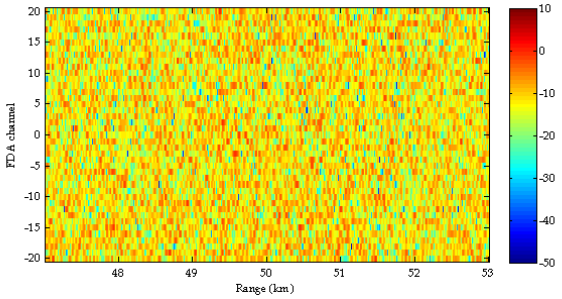

Figure 3: The simulated single-pulse received raw data in FDA channels prior to pulse compression (a noise-dominated image, –10 dB SNR in raw data).

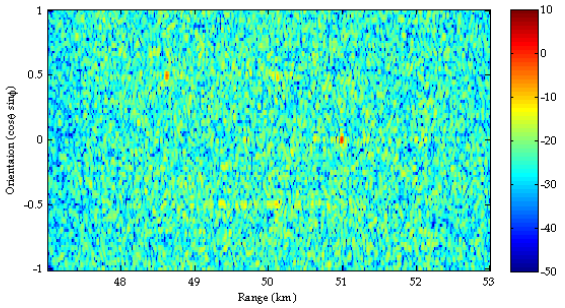

Figure 4: After pulse compression by the range-unambiguous matched filter (the current pulse) and beamforming, Targets 1 and 2 are focused and detected, and Target 3 becomes an interference signal.

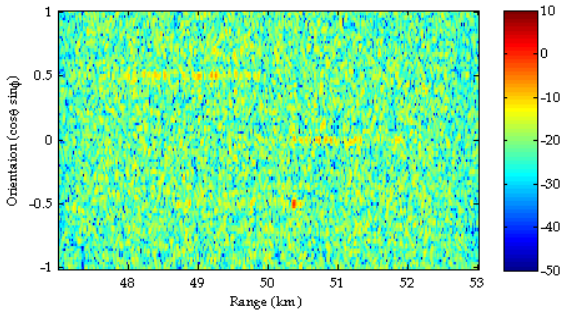

Figure 5: After pulse compression by the range-ambiguous matched filter (the previous pulse) and beamforming: Target 3 is focused and detected, and Targets 1 and 2 become interference signals.

In order to search out any targets in ambiguous range, the raw dataset was reprocessed using the previous pulse as the

matched filter, and the result is shown in Figure 5. It can be seen that in this case Target 3 ($r = 50.375$ km and $\cos\theta\sin\phi = -0.5$) is focused and detected whereas Targets 1 and 2 become interference signals. Since Target 3 is off the boresight direction, the associated range shift in time, according to (10) is $-2.5\,\mu$s, i.e. -0.375 km in range. Therefore, the apparent range of Target 3 should be 50 km. Because PRF is 1500 Hz, the true range of Target 3 is 150 km, consistent with the given simulation parameters.

The isolation among pulses is limited by the lower boundary of the cross-correlation of the pulses as discussed. If the isolation level is not satisfied to the system design, other techniques or algorithms need to be considered. One technique is using the frequency-division multiple access (FDMA) pulse by pulse. Another possible solution is to use signal-removal algorithms. Once a target (especially those strong ones) is detected, its signal is synthesised and removed from the original raw data to eliminate its interference to weak targets.

A single CPA pulse data can only produce a 1D range profile and a CPI burst of pulse train data can produce a 2D range-Doppler map. However, for the FDA data, a single pulse data can produce multiple 2D range-orientation maps (range-unambiguous, first-order range-ambiguous, etc) and a CPI burst of pulse train data can produce multiple 3D range-orientation-Doppler maps.

The concept of space-time adaptive processing (STAP) can be adapted to processing the FDA data, which is out of the scope of this paper.

V. CONCLUSIONS

The focus of this paper is more at details of how the FDA data should be systematically and efficiently processed, which was largely missing in the previous publications. The detection and identification of range-ambiguous targets by the FDA radar without using multiple PRFs is demonstrated.

The non-coherent emission enables the FDA radar detection without using electronic scan that greatly simplifies the radar design and operation. Hence, the FDA has a great potential to be implemented in simple wide-area search radars and navigation radars without compromising its performance.

Once the FDA CW waveform are coded with an initial random phase as defined by (18), the pulse becomes a noise-like one with varying amplitude and phase. It makes the FDA radar low probability of interception and difficult to be jammed.

Because of energy spread, the energy emitted onto a target is $10\log_{10}(N+1)$ dB less than that of CPA radar. The FDA radar may be not quite suitable for the long-range detection. Therefore, in comparison with the conventional phased-array (CPA) radar, the detection area is fan-area like for the former and pencil-beam like for the latter making two radars (or radar operation modes) complementary.

REFERENCES

[1] P. Antonik, M. C. Wicks, H. D. Griffiths and C. J. Backer: "Frequency Diverse Array Radars", *Proceedings of IEEE Radar Conference*, (2006)

[2] P. Antonik, M. C. Wicks, H. D. Griffiths and C. J. Backer: "Range-Dependent Beamforming Using Element Level Waveform Diversity", *Proceedings of International Waveform Diversity and Design Conference*, (2006)

[3] P. Baizert, T. B. Hale, M. A. Temple and M. C. Wicks: "Forward-Looking Radar Gmti Benefits Using a Linear Frequency Diverse Array," *Electronics Letters*, 42, (22),2006, pp. 1311-1312

[4] P. F. Sammartino, C. J. Backer and H. D. Griffiths: "Frequency Diverse Mimo Techniques for Radar," *IEEE Trans on Aerospace and Electronic Systems*, 49, (1),2013, pp. 201-222

[5] J. Liang and Q. Liang: "Orhogonal Waveform Design and Performance Analysis in Radar Sensor Networks", *Proceedings of the 2006 IEEE Conference on Military Communications*, (2006)

[6] Q. Liang: "Waveform Design and Diversity in Radar Sensor Networks: Theoretical Analysis and Application to Automatic Target Recognition", *Proceedings of IEEE International Worshop on wireless ad hoc and sensor networks*, (2006)

[7] W. Khan and I. M. Qureshi: "Frequency Diverse Array Radar with Time-Dependent Frequency Offset," *IEEE Antennas and Wireless Propagation Letters*, 13,2014, pp. 758-761

[8] D. W. Bliss, K. W. Forsythe, S. K. Davis, G. S. Fawcett, D. J. Rabideau, L. L. Horowitz and H. Kraut: "Gmti Mimo Radar", *Proceedings of the 2009 International WD&D Conference*, (2009)

[9] J. J. Zhang and A. Papandreou-Suppappola: "Mimo Radar with Frequency Diversity", *Proceedings of the 2009 International WD&D Conference*, (2009)

[10] W.-Q. Wang: "Overview of Frequency Diverse Array in Radar and Navigation Applications," *IET Radar, Sonar and Navig.*, 10, (Iss 6),2016, pp. 1001-1012

[11] W.-Q. Wang: "Frequency Diverse Array Antenna: New Opportunities," *IEEE A&E Systems Magazine*, 57, (2),2015, pp. 145-152

[12] J. J. Huang, K. F. Tong and C. J. Backer: "Frequency Diverse Array with Beam Scanning Feature", *Proceedings of IEEE Antennas and Propagation Society International Symposium* (2008)

[13] W. Q. Wang: "Range-Angle Dependent Trasmit Beampattern Synthesis for Linear Frequency Diverse Arrays," *IEEE Trans on Antennas and Propagation*, 61, (8),2013, pp. 4073-4081

[14] Y. Dong: "Frequency Diverse Radar and Its Data Processing," *IET Radar, Sonar and Navig.*,Under review, 2018

[15] L. R. Welch: "Lower Bounds on the Maximum Cross Correlation of Signals," *IEEE Trans on Inf. Theory*, IT-20, (3),1973, pp. 397-399